

## Differences in the composition of hip and knee synovial fluid in osteoarthritis: a nuclear magnetic resonance (NMR) spectroscopy study of metabolic profiles



P. Akhbari <sup>† \*</sup>, M.K. Jaggard <sup>†</sup>, C.L. Boulangé <sup>§</sup>, U. Vaghela <sup>||</sup>, G. Graça <sup>§</sup>, R. Bhattacharya <sup>†</sup>, J.C. Lindon <sup>§</sup>, H.R.T. Williams <sup>† a</sup>, C.M. Gupte <sup>† a</sup>

<sup>†</sup> Department of Orthopaedics & Trauma, Imperial College Healthcare NHS Trust, London, United Kingdom

<sup>‡</sup> Department of Digestive Diseases, Imperial College Healthcare NHS Trust, London, United Kingdom

<sup>§</sup> Department of Metabolism, Digestion and Reproduction, Imperial College London, London, United Kingdom

<sup>||</sup> School of Medicine, Imperial College London, London, United Kingdom

### ARTICLE INFO

#### Article history:

Received 3 July 2018

Accepted 3 July 2019

#### Keywords:

Metabolic profiling  
Metabonomics  
NMR  
Osteoarthritis  
Synovial fluid

### SUMMARY

**Objective:** The hip and knee joints differ biomechanically in terms of contact stresses, fluid lubrication and wear patterns. These differences may be reflected in the synovial fluid (SF) composition of the two joints, but the nature of these differences remains unknown. The objective was to identify differences in osteoarthritic hip and knee SF metabolites using metabolic profiling with Nuclear Magnetic Resonance (NMR) spectroscopy.

**Design:** Twenty-four SF samples (12 hip, 12 knee) were collected from patients with end-stage osteoarthritis (ESOA) undergoing hip/knee arthroplasty. Samples were matched for age, gender, ethnicity and had similar medical comorbidities. NMR spectroscopy was used to analyse the metabolites present in each sample. Principal Component Analysis and Orthogonal Partial Least Squares Discriminant Analysis were undertaken to investigate metabolic differences between the groups. Metabolites were identified using 2D NMR spectra, statistical spectroscopy and by comparison to entries in published databases.

**Results:** There were significant differences in the metabolic profile between the groups. Four metabolites were found in significantly greater quantities in the knee group compared to the hip group (N-acetylated molecules, glycosaminoglycans, citrate and glutamine).

**Conclusions:** This is the first study to indicate differences in the metabolic profile of hip and knee SF in ESOA. The identified metabolites can broadly be grouped into those involved in collagen degradation, the tricarboxylic acid cycle and oxidative metabolism in diseased joints. These findings may represent a combination of intra and extra-articular factors.

© 2019 Osteoarthritis Research Society International. Published by Elsevier Ltd. All rights reserved.

### Introduction

Osteoarthritis (OA) most commonly involves the hip and knee joints, and treatment of this condition leads to significant social and economic costs<sup>1</sup>. The aetiology of OA is multifactorial, but the final pathway results in progressive degradation of chondral cartilage and may involve synovial inflammation and changes to the sub-chondral bone. This wear of intra-articular tissues results in metabolites in the synovial fluid (SF) that represent inflammatory and degradation products<sup>2</sup>.

Hip and knee joints have different biomechanical profiles<sup>3,4</sup>. Thus, the wear patterns in these joints is different both clinically and radiologically. This may in turn lead to differences in the fluid metabolites related to these wear patterns, although there is

\* Address correspondence and reprint requests to: P. Akhbari, Department of Trauma and Orthopaedics Imperial College NHS Trust Praed Street St Mary's Hospital Salton House London, W2 1NY United Kingdom. Tel.: 44-20-33121930; fax: 44-20-33121471.

E-mail addresses: [pakhbari@nhs.net](mailto:pakhbari@nhs.net) (P. Akhbari), [m.jaggard@nhs.net](mailto:m.jaggard@nhs.net) (M.K. Jaggard), [c.boulange09@imperial.ac.uk](mailto:c.boulange09@imperial.ac.uk) (C.L. Boulangé), [uddhav.vaghela14@imperial.ac.uk](mailto:uddhav.vaghela14@imperial.ac.uk) (U. Vaghela), [g.gomes-da-graca@imperial.ac.uk](mailto:g.gomes-da-graca@imperial.ac.uk) (G. Graça), [rajarshi.bhattacharya@imperial.ac.uk](mailto:rajarshi.bhattacharya@imperial.ac.uk) (R. Bhattacharya), [j.lindon@imperial.ac.uk](mailto:j.lindon@imperial.ac.uk) (J.C. Lindon), [h.williams@imperial.ac.uk](mailto:h.williams@imperial.ac.uk) (H.R.T. Williams), [c.gupte00@imperial.ac.uk](mailto:c.gupte00@imperial.ac.uk) (C.M. Gupte).

<sup>a</sup> H.R.T. Williams and C.M. Gupte are joint senior authors.

limited evidence of this<sup>2,5–7</sup>. Several studies have demonstrated differences in cytokine, enzyme and protein concentrations of SF between these joints<sup>5–7</sup>.

Metabolic profiling is a novel technique, which studies the low molecular weight metabolites within a cell, tissue or biofluid using either mass spectrometry (MS) or nuclear magnetic resonance (NMR) spectroscopy. Its potential lies in the ability to analyse hundreds or even thousands of small molecules simultaneously. This technique has been employed in several conditions to influence clinical practice<sup>8–10</sup>. More recently, it has been used to identify metabolites within the urine, blood and SF of both animal models and in humans with OA<sup>11,12</sup>. This has yielded not only individual biomarkers for a specific pathological process, but also unique metabolic “signatures” consisting of many metabolites that may identify a distinct pathology based on relative concentrations of these molecules<sup>13</sup>.

Although recent developments in the field of metabolic profiling have improved the detection of small molecules in various biological tissues and fluids, there are few studies examining the small molecule composition of human SF (HSF)<sup>12,14–19</sup>. The majority of these have used MS, which has good sensitivity. However, MS is limited by variable ionisation and ion suppression effects, which impair analyte detection<sup>20</sup> and involves destruction of the samples such that repeat testing is precluded. Furthermore, in order to improve metabolite resolution, MS is usually coupled with prior separation of the fluid using chromatography or capillary electrophoresis.

Whilst NMR spectroscopy has a lower sensitivity and a sparser metabolite coverage than MS, its strengths lie in universality of detection, ease of quantitation and the ability to annotate spectral features. It is fast and non-destructive allowing multiple samples to be measured in a day, and the same sample can be analysed numerous times, unlike with MS<sup>20</sup>.

Previous analysis of SF has led to a better understanding of the metabolic processes associated with OA and also led to the identification of some of the biomarkers of OA such as arginine and the ratio of branched chain amino acids (BCAAs) to histidine<sup>12,19,21,22</sup>. However, these studies have examined hip and knee SF as a homogeneous group<sup>12,14–19</sup>. There are currently no studies in the literature utilising NMR spectroscopy to assess the differences in small molecule composition between hip and knee SF.

## Aims and hypothesis

Our hypothesis was that there were differences in the metabolic composition of SF of end-stage osteoarthritic hip and knee joints. The aim of this study was therefore to identify these differences using NMR spectroscopy.

## Materials and methods

Ethical approval was granted by our local research ethics committee (Project 15/LO/0388) and all patients gave informed consent to participate in this study. From the available samples, patients were matched exactly for gender and within 5 units for body mass index (BMI) and 5 years for age. From this cohort, patients with similar medical comorbidities were selected in an attempt to remove these as confounding factors. SF was harvested from 24 patients undergoing primary hip (12 patients) or knee (12 patients) arthroplasty for end-stage osteoarthritis (ESOA) at our institution. ESOA was confirmed based on the patient's symptoms,

radiographs and intraoperative findings. All patients completed a questionnaire, which included information on demographics, diet, lifestyle, medical co-morbidities, medications, duration and severity of symptoms and previous intra-articular injections. Comorbidities included metabolic-related diseases (diabetes, hypertension, ischaemic heart disease, gout, osteoporosis, raised cholesterol and stroke). Data was also collected from the patient's records on BMI.

### Sample preparation and metabolic profiling

Samples were collected intraoperatively using a standardised protocol. The knee joint was approached using a midline incision and medial parapatellar approach, whilst a posterior approach was used for the hip<sup>23</sup>. Following skin incision but prior to hip capsulotomy/knee arthrotomy, a 14G syringe was inserted into the suprapatellar pouch of the knee/along the femoral neck of the hip and SF was aspirated. The sampling technique was similar between the groups. Samples were aliquoted and centrifuged at 10,000 g for 15 min. The supernatant was aliquoted, thus removing any cellular material or debris. All samples were stored at -80°C for a maximum of 6 months before analysis.

Samples were defrosted no more than 1 h before being assayed. Each sample (400 µl) was combined with an equal amount of 75 mmol/L sodium dihydrogen phosphate (NaH<sub>2</sub>PO<sub>4</sub>) buffer at pH 7.4 containing 6.2 mmol/L sodium azide (NaN<sub>3</sub>) and 4.6 mmol/L of 3-(trimethylsilyl)-2,2,3,3-tetradeutero propionic acid sodium salt (TSP) and 20% deuterium oxide (D<sub>2</sub>O) as published by Dona et al.<sup>24</sup>

Control samples containing only buffer were run in tandem with the HSF samples to identify and exclude potential contamination, which may have occurred at any stage during sample preparation.

Experiments were performed using a Bruker® Avance III 600 MHz spectrometer with a Samplejet 96 well autosampler. One dimensional (1D) high resolution NMR (<sup>1</sup>H-NMR) spectra were acquired for each sample using the NOESY 1D pulse sequence with optimised water presaturation, as a sum of 128 free induction decays, with 128 k complex points, a mixing time of 10 ms, a delay between the two 90 radiofrequency pulses of 4 µs and a relaxation time of 4 s.

NMR spectral chemical shifts were internally referenced to glucose (5.23 ppm), automatically phased and baseline corrected. An exponential function was applied to the NMR FIDs prior to being Fourier transformed providing a line broadening of 0.3 Hz, using Topspin 3.2 (Bruker, Germany). The NMR spectra were then imported into Matlab™ (Matlab2016b, Mathworks, Massachusetts, United States) and consisted of 27,492 data points. Spectra were aligned according to the method developed by Veselkov et al. to allow comparison of peaks between samples<sup>25</sup>. A median-fold change normalisation method was used to normalise the spectra<sup>26</sup>. Following normalisation, the data was scaled to unit variance<sup>27</sup>.

### Metabolite identification

Metabolite identification was achieved by matching chemical shift and peak multiplicity with information in the literature and databases (Human Metabolome Database<sup>28</sup>, Biological Magnetic Resonance Bank<sup>29</sup>). Statistical total correlation spectroscopy (STOCSY)<sup>30</sup> was used to aid metabolite identification by

demonstrating peaks (or variables), which show statistical correlations with other peaks (or variables) in the spectra, and thus belong to the same molecule or originate from another molecule related functionally<sup>30</sup>. Two-dimensional NMR spectra, namely  $^1\text{H}$ – $^1\text{H}$  total correlation spectroscopy (TOCSY) and  $^1\text{H}$ – $^{13}\text{C}$  heteronuclear single-quantum correlation spectroscopy (HSQC), were acquired for representative samples to further confirm the identified metabolites.

### Statistical analysis

To analyse the large dataset (27,492 variables per sample) generated by NMR, Principal Component Analysis (PCA) and Orthogonal Partial Least Squares-Discriminate Analysis (O-PLS-DA), are the most prominent multivariate analysis techniques<sup>31</sup>. The different data points of the NMR spectra can be thought of being part of a multidimensional graph representing “metabolic coordinates”. A more detailed explanation can be found in the article by Lindon et al.<sup>20</sup> and in [Appendix 1](#). Analysis was performed using the SIMCA 14™ statistical package (Sartorius Stedim Biotech, Umea, Sweden). PCA provides an overview of the samples, highlights clustering, and identifies outliers. O-PLS-DA modelling was used to further investigate the differences between the groups. In this method, we regress the NMR data (X matrix) against class variables for the two groups or Y variable. The Y variable is a numerical vector, which encodes the group information. Using this procedure, we identified differences between the two groups. In order to assess the model validity, seven-fold cross validation was performed. The parameters  $Q^2\text{Y}$  and  $R^2\text{Y}$  were evaluated as measures of model fitting. The goodness of prediction ( $Q^2\text{Y}$ ) measures the predictability of the model. The goodness of fit ( $R^2\text{Y}$ ) is the proportion of the NMR data that explains the differences between the two groups (Y variable). The robustness of the model was assessed by calculating the  $Q^2\text{Y}$  100 times by randomly assigning the cross-validation groups (the samples predicted in each of the seven cross-validation rounds). The  $Q^2\text{Y}$  values were compared with  $Q^2\text{Y}$  values obtained after performing 100 permutations of the Y variable. The model was considered reliable if the  $Q^2\text{Y}$  confidence intervals of the permuted and non-permuted models did not overlap.

The metabolite signals responsible for the separation between the two groups were identified from the O-PLS-DA model loadings plot. The O-PLS-DA separates the data into predictive components that explains the differences between the two groups and the orthogonal component that contains the remaining unrelated information. Only signals with a correlation coefficient to the Y variable  $>0.6$  were considered to have a significant impact on group separation. To better identify the peaks, back transformation of the loadings was performed by multiplying each variable by its standard deviation. The NMR signals related to the predictive components are then integrated to demonstrate the differences between the two groups for the identified metabolites. The individual peaks of all the spectra were also visualised to see if there were any obvious differences between the two groups. The area under each metabolite peak was analysed by univariate analysis, using the Student's t-test.

The false discovery rate (FDR) adjusted  $p$ -values were calculated using the Benjamini-Hochberg method<sup>32</sup> and was performed to account for multiple testing of the identified metabolites. Network analysis was performed on the identified metabolites to further the

**Table I**

Patient demographics. There was no significant difference in age ( $P = 0.27$ ), gender, BMI ( $P = 0.71$ ) or medical co-morbidities between the groups. IHD, Ischaemic heart disease; DM, Diabetes Mellitus; CVA, Cerebrovascular Accident

	Hip	Knee
Number of patients	12	12
Age (Mean $\pm$ SD)	67.7 (12.2)	63.3 (21.2)
Gender (Male: Female)	3:9	3:9
BMI (Mean $\pm$ SD)	30.4 (5.1)	29.9 (4.6)
Ethnicity	11 Caucasian 1 Asian	9 Caucasian 2 Afro-Caribbean 1 Asian
Disease (Number of patients per group)		
IHD	2	0
Hypertension	9	8
Hypercholesterolaemia	7	6
DM	4	2
CVA	1	0

interpretation of metabolic changes, using the MetaboNetworks software in Matlab™<sup>33</sup>.

## Results

### Patient demographics

There were no significant differences in age ( $P = 0.27$ ), gender or BMI ( $P = 0.71$ ) between the groups and the common medical co-morbidities were also similar ([Table I](#)). Two hip and three knee patients had received a steroid injection. One injection in the knee group was performed 6 months before the HSF sample was taken and the remaining four injections were performed over a year before the samples were taken. None of the patients had received a synthetic hyaluronic acid injection. The full list of medical co-morbidities and medications are included in [Appendix 2](#).

### PCA and O-PLS-DA analysis of differences between hip and knee metabolites

A typical  $^1\text{H}$ -NMR spectra of hip and knee SF from the current cohort is demonstrated in [Fig. 1](#). The PCA scores plot ([Fig. 2](#)) demonstrated some separation between the  $^1\text{H}$ -NMR spectra in the hip and knee groups in PC1 (24%). This suggested that there may be metabolic differences in the HSF composition of the two joints. Although PC2 (15%) and PC3 (11%) are still associated with variability within the data, no separation is observed in the scores of those components ([Fig. 2](#) and [Appendix 3](#)). The knee group demonstrated tighter clustering whereas the hip group showed more variability based on the NMR spectra of HSF. Further inspection of the PCA scores plots showed that the heterogeneity of the hip group is not motivated by age, gender or BMI ([Appendix 4](#)).

By using seven-fold cross-validation, an O-PLS-DA model with good predictive ability was obtained ( $Q^2\text{Y} = 0.360$  [95% CI 0.348–0.373],  $R^2\text{Y} = 0.873$ ). This was further confirmed by running permutation analyses on the model ( $Q^2\text{Y} = 0.234$  [95% CI -0.298 to -0.170] and  $R^2\text{Y} = 0.705$  [95% CI was 0.693–0.716]) [[Fig. 3\(a\)](#)]. O-PLS-DA analysis showed separation between hip and knee SF [[Fig. 3\(b\)](#)] and allowed identification of the metabolite resonances, which were responsible for the separation of the hip and knee

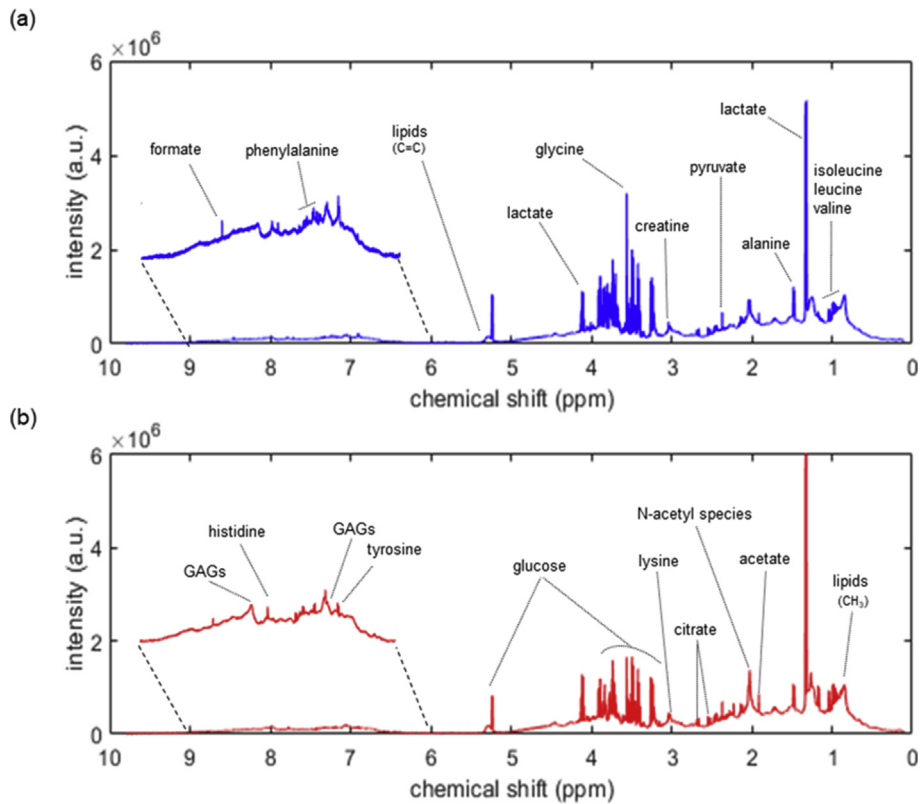


**Fig. 1.** Typical  $^1\text{H}$ -NMR spectra taken from the study cohort demonstrating some of the identified metabolites. a. Knee synovial fluid. b. Hip synovial fluid. GAGs – glycosaminoglycans.

groups through inspection of the back-scaled O-PLS-DA loadings plot.

All the metabolites consistently identified in all samples are listed in [Appendix 5](#). HSF from the knee group showed greater levels of alanine, citrate, dimethylsulfone, glucose, glutamine, glycosaminoglycans (GAGs), histidine, lysine, N-acetylated molecules, pyruvate and valine compared to the hip group. HSF from the hip group showed greater levels of choline compared to the knee group [[Fig. 4\(a\) and \(b\)](#)].

#### Evaluation of individual spectra

The individual spectral analysis confirmed the metabolic differences identified from the back-scaled loadings plot of the O-PLS-DA and additionally revealed greater quantities of tyrosine in the knee and hypoxanthine in the hip group ([Fig. 5](#)). All the metabolites identified that were found in different quantities between the 2 groups are listed in [Table II](#). Following FDR adjustment of the  $p$ -values, four of these metabolites remained significant ([Table II](#)).

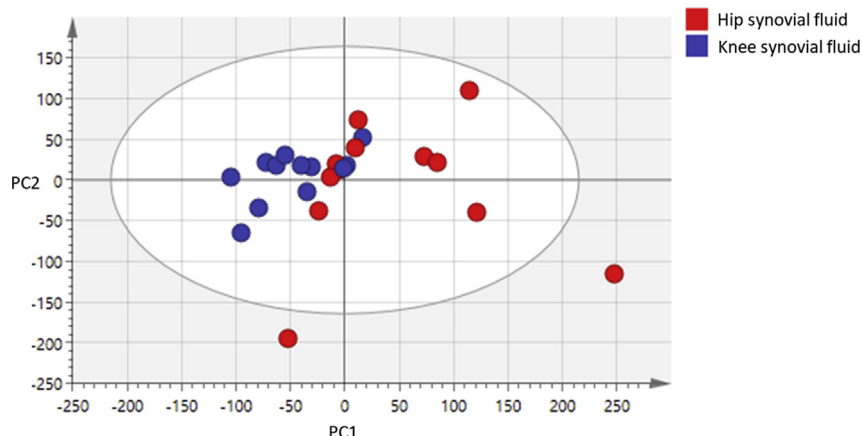


**Fig. 2.** PCA scores plot of PC1 vs PC2 with each data point representing the NMR spectrum of an individual human synovial fluid sample and demonstrating separation between the hip and knee groups. The ellipse represents Hotelling T2 with 95% confidence interval. The percentage variation explained is 24% for PC1 and 15% for PC2. PC – principal component.

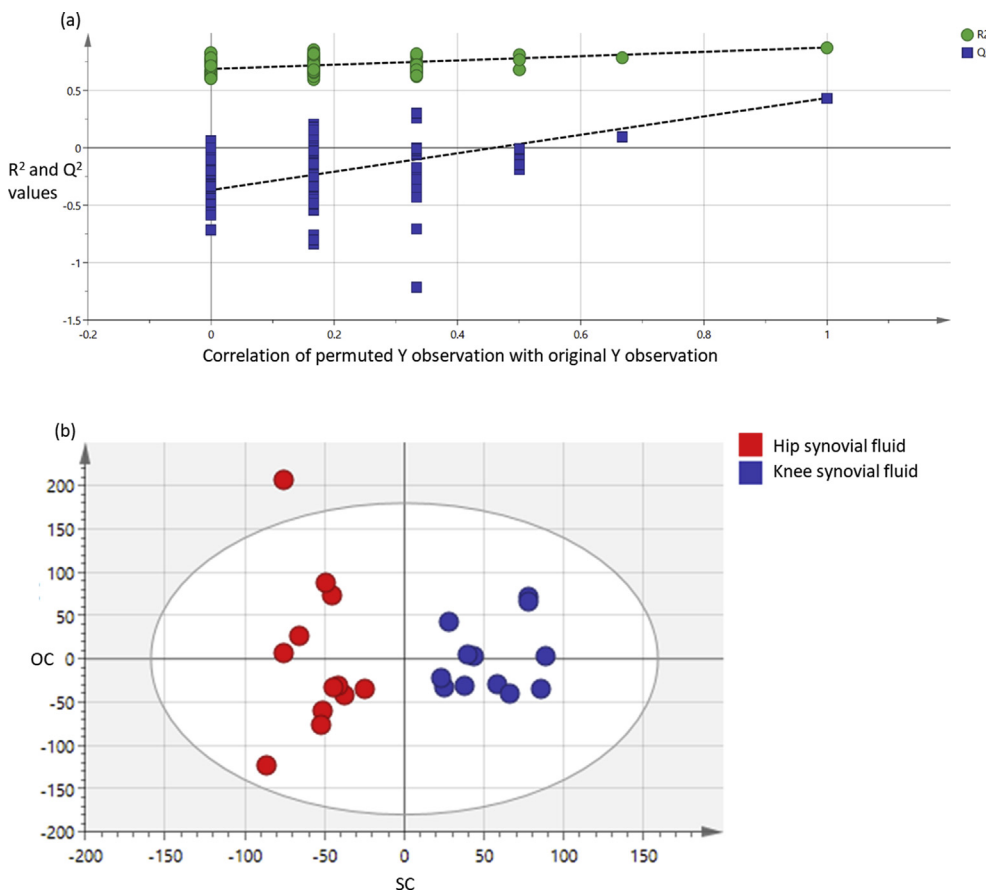


**Fig. 3.** O-PLS-DA model of osteoarthritic SF comparing hip and knee groups. a. Graphical representation of the permutation analysis demonstrating that all the permuted models have a Q<sup>2</sup>Y value lower than the values obtained in the hip vs knee synovial fluid model. b. Scores plot of the cross-validated O-PLS-DA model demonstrated a good separation between the hip and knee groups with differences in the spectra of each sample explained by whether the fluid was taken from the hip or knee joint. The ellipse represents Hotelling T<sup>2</sup> with 95% confidence interval. SC – separating component; OC – orthogonal component.

**Table II**  
Metabolites identified from the back-scaled loadings, univariate analysis and confirmed by 2D-NMR spectra. Following FDR adjustment, only four of the 14 identified metabolites remained significant and they were all found in greater quantities in the knee group (\*). The chemical shift indicates which metabolite peaks were integrated and used for metabolite comparison between the two groups. The peak area for the two cohorts is also provided, but the units are arbitrary and hence not included. GAG – glycosaminoglycans; ppm – parts per million; 95%CIs – 95% confidence intervals; FDR – false discovery rate

Metabolite ID	NMR chemical shift (ppm)	Joint containing higher concentration of metabolite	Peak area: knee cohort (mean [95%CIs])	Peak area: hip cohort (mean [95%CIs])	P-value (Student's t-test)	FDR-adjusted P-value
N-Acetylated molecules*	2.02	knee	1,674.9 [1365.6–1984.1]	625.7 [386.7–864.7]	0.000034	0.001
GAG*	7.97	knee	2,615.1 [2,352.4–2,877.8]	1,669.9 [1371.6–1968.2]	0.00012	0.004
Citrate*	2.53	knee	1,243.2 [1065.2–1421.2]	766.1 [639.4–892.7]	0.00037	0.012
Glutamine*	2.45	knee	2,759.4 [2,366.2–3,152.6]	1,837.5 [1622.2–2052.8]	0.0009	0.028
Hypoxanthine	8.18	hip	33.7 [27.8–39.5]	54.8 [44.2–65.5]	0.003	0.110
Dimethylsulfone	3.15	knee	139.8 [104.0–175.5]	71.8 [50.1–93.5]	0.005	0.167
Tyrosine	7.19	knee	254.8 [207.6–301.9]	166.8 [139.0–194.6]	0.006	0.183
Lysine	3.03	knee	608.2 [540.3–676.0]	483.4 [444.0–522.8]	0.006	0.200
Choline	3.19	hip	160.5 [130.2–190.8]	254.8 [203.7–305.9]	0.006	0.200
Pyruvate	2.37	knee	529.8 [444.3–615.3]	350.6 [259.4–441.8]	0.010	0.339
Valine	1.04	knee	1,506.4 [1219.2–1793.7]	1,047.8 [924.1–1171.6]	0.012	0.384
Glucose	5.23	knee	4,113.4 [3,448.2–4,778.6]	2,742.3 [2000.9–3,483.6]	0.013	0.436
Histidine	7.05	knee	166.3 [139.2–193.4]	125.7 [113.6–137.9]	0.017	0.566
Alanine	1.47	knee	2,666.4 [2,121.0–3,211.8]	1,829.8 [1452.1–2,207.5]	0.023	0.751

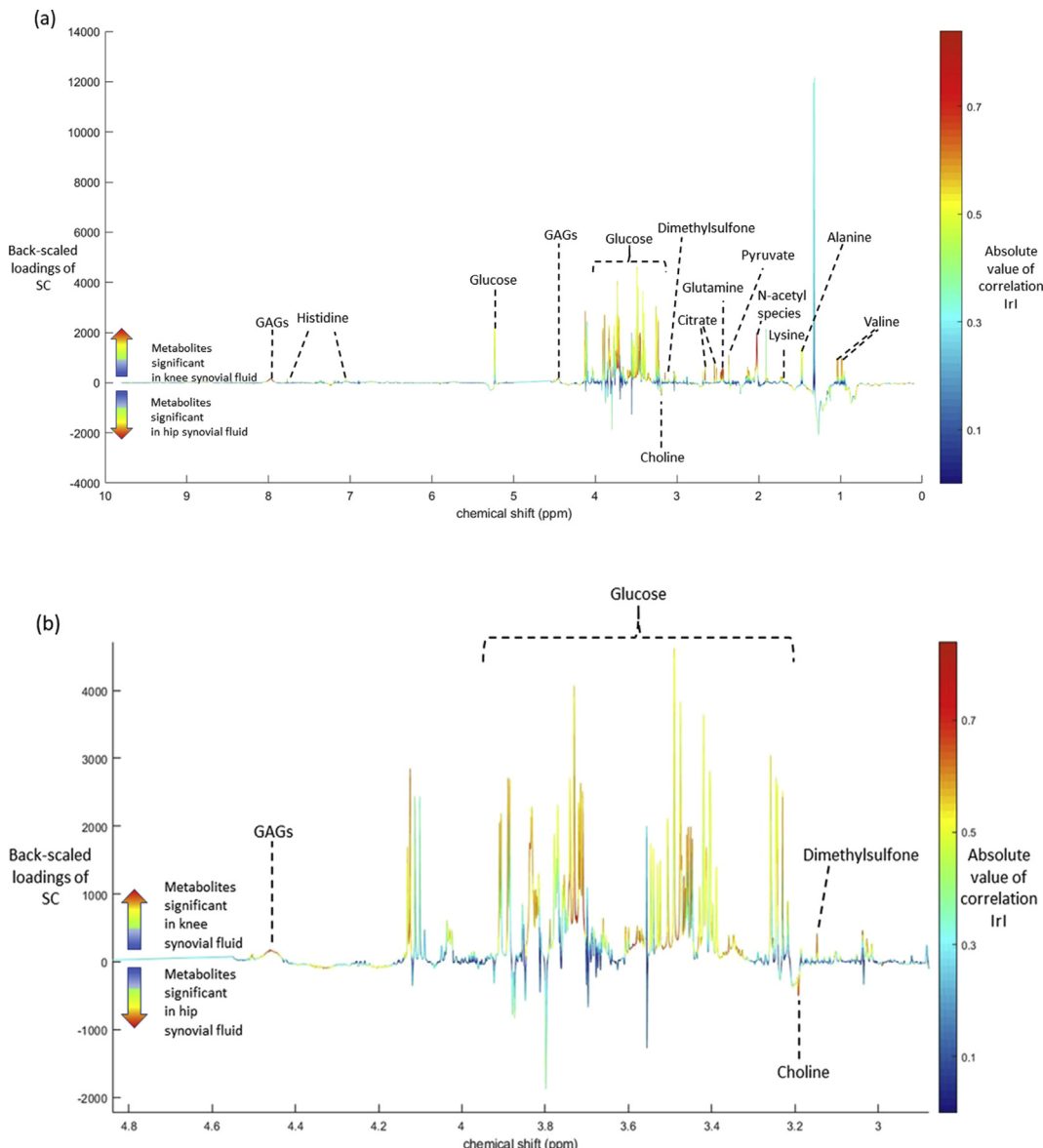


**Fig. 4.** Back-scaled loadings plot of SC from the O-PLS-DA model. a. The significant metabolites are red peaks, with those pointing upwards significantly increased in knee and those pointing downwards significantly increased in hip synovial fluid. b. Expansion of the Back-scaled loadings plot demonstrating the difference between the glucose and choline peaks. GAGs – glycosaminoglycans; SC – separating component; ppm – parts per million.

These were N-acetylated molecules, GAGs, citrate and glutamine. A network analysis of all the identified metabolites was created and is included in [Appendix 6](#).

## Discussion

SF of hips and knees with end-stage OA (ESOA) was examined for small metabolites using NMR spectroscopy. After appropriate statistical analysis (PCA, O-PLS-DA, FDR adjustment of *P*-values), there were significant differences in four metabolites (N-acetylated molecules, GAGs, citrate and glutamine), which were found in greater quantities in knee SF.

FDR analysis ensures that detected differences are unlikely to be due to chance, but this can lead to false negatives when small numbers of samples are used. For this reason, the remaining metabolites are also considered in the discussion. Eight further metabolites (alanine, dimethylsulfone, glucose, histidine, lysine, pyruvate, tyrosine and valine) were found in

greater proportion in the knee group and two metabolites (choline and hypoxanthine) were found in greater proportion in the hip group. The possible functions of these metabolites are listed in [Appendix 7](#).

This is the first study to examine the metabolic differences in HSF between the hip and knee joints in patients with ESOA. All the identified metabolites can broadly be grouped into those involved in proteoglycan (PG) and collagen degradation, the tricarboxylic acid (TCA) cycle, lipid metabolism and BCAA catabolism.

## Analysis of metabolite differences

[Table III](#) lists the possible functions of the four metabolites, which remained significant following FDR adjustment.

GAGs are typically found in the extracellular matrix (ECM)<sup>34</sup>. They attach to a core protein leading to the formation of PGs. Due to their important role in maintaining the turgor pressure of articular

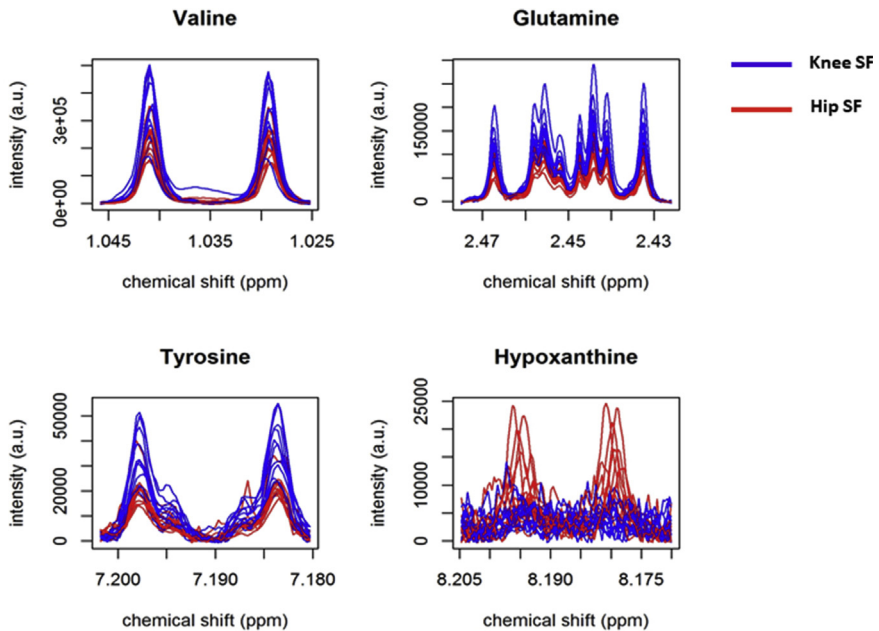


**Fig. 5.** Metabolite analysis from spectral inspection. Figure demonstrates differences in signal intensity between the groups. Valine & glutamine were identified from the back-scaled loadings but have been inserted to demonstrate they still show a difference between the groups on spectral inspection. Tyrosine & hypoxanthine did not show significant differences on the back-scaled loadings, but the differences are apparent when comparing the individual spectra. SF – synovial fluid; ppm – parts per million.

cartilage<sup>35</sup>, the greater proportion of GAGs in the knee group suggests a greater rate of articular cartilage breakdown compared to the hip group. This results in altered tribological and mechanical responses, ultimately leading to matrix degradation<sup>36</sup>. As hyaluronic acid (HA) is the principal N-acetyl-glucosamine containing polymer in SF, a greater intensity of the N-acetylated molecule signal in the knee group suggests greater PG and hence cartilage degradation<sup>37</sup>.

Citrate is a major intermediary in the TCA cycle, urea cycle, amino acid and fatty acid metabolism<sup>38</sup>. The TCA cycle is a key biochemical pathway that provides cellular energy in the form of Adenosine Triphosphate (ATP) by oxidative conversion of carbohydrates. Most of carbon contributes to the TCA cycle through the conversion of glucose to pyruvate, but there is also a contribution of glutamine to the TCA intermediary alpha-ketoglutarate. Glutamine has an important role in oxidative metabolism, and therefore elevated levels suggest altered oxidative metabolism in diseased joints<sup>39</sup>. Our results agree with other studies, demonstrating that alterations in the metabolic profile of SF from OA patients also suggests a role for altered energy metabolism in OA<sup>15,17,21</sup>. The greater abundance of TCA intermediaries in the knee group could also be related to mitochondrial dysfunction, where the TCA cycle functions<sup>40</sup>.

A network analysis of all the identified metabolites was performed, including those that did not survive FDR correction (Appendix 6). This illustrates several different pathways involved in hip (phospholipid metabolism via choline) and knee (amino acids, TCA and glucose metabolism) osteoarthritic HSF metabolism. This correlates with the potential functions of these metabolites described above and in Appendix 7.

#### Possible causes of differences in hip and knee synovial fluid metabolites

It is important to realise that OA is a heterogenous syndrome with various aetiopathogenic phenotypes. Therefore, a more integrated approach is required when thinking about the pathological

processes involved in this condition. This remains true when considering the metabolic differences between the hip and knee groups. Broadly speaking, these differences may be due to or a combination of intra and extra-articular factors.

The hip has classically been thought of as a ball and socket joint with a high level of conformity<sup>3</sup>. On the other hand, the knee joint is less conforming with greater contact stresses, due to a smaller area of contact between the tibio-femoral articulations. One of the functions of the meniscus is to increase the contact area in the knee to help distribute joint forces to a larger surface area than the direct tibio-femoral cartilage contact region<sup>4</sup>. However, in severe knee OA, the meniscus does not always function normally due to meniscal tears or calcification, thus reducing its ability to act in this capacity. Consequently, there may be greater point loading in the knee resulting in a larger force through a smaller area, whereas in the hip there is a more volumetric wear pattern due to the greater conformity. In addition, SF incorporates metabolites from the surrounding tissues within the joint, as well as systemic sources. Synovial inflammation in OA may have an important role. There are numerous pathways and mediators, which may be responsible, including proinflammatory mediators, such as interleukin-10 (IL-10) and transforming growth factor- $\beta$  (TGF- $\beta$ ), and matrix metalloproteinases, ultimately resulting in changes to the metabolic profile of SF<sup>41</sup>. Mitochondrial activity has also been shown to increase when exposed to osteoarthritic SF<sup>41</sup>. Furthermore, plasma and SF bone morphogenic protein-2 (BMP-2) levels have been positively correlated to the severity of knee OA<sup>42</sup>. Cartilage turnover has been demonstrated to be significantly greater in the knee than the hip, suggesting different mechanisms of disease progression between these joints<sup>43</sup>. This was felt to be due to differences in protein turnover, more specifically, the attempted cartilage repair response.

Extra-articular factors include age, BMI and medical comorbidities. Obesity has been linked to OA in both the hip and knee, but its effect is more profound in the knee joint<sup>44</sup>. However, in this study, patients were matched for age and BMI in attempt to

**Table III**

List of identified metabolites, the joint in which they are found in significantly greater quantities and the function of the metabolites in osteoarthritis. GAGs – glycosaminoglycans; NO – Nitric Oxide; PG – proteoglycan; TCA tricarboxylic acid

Metabolite ID	Joint containing larger quantity of metabolite	Function of metabolite	Reference
N-Acetylated molecules	knee	Marker of PG breakdown & cartilage degradation.	Schiller et al. <sup>34</sup>
GAGs	knee	Marker of articular cartilage breakdown.	Thompson et al. <sup>35</sup>
Citrate	knee	Major intermediary in the TCA cycle, urea cycle, amino acid & fatty acid metabolism. Role in altered energy metabolism with elevated levels suggesting altered oxidative metabolism in diseased joints.	Berg et al. <sup>36</sup>
Glutamine	knee	Key role in oxidative metabolism. Elevated levels suggest altered oxidative metabolism in diseased joints. It also suppresses the formation of inflammatory cytokines and protects chondrocytes from NO induced apoptosis and heat stress.	Kim et al. <sup>16</sup> Handley et al. <sup>37</sup> Kim et al. <sup>38</sup> Tonomura et al. <sup>39</sup>

remove these as confounding factors. Similarly, there were comparable medical co-morbidities in both groups to reduce their effects as potential confounding factors.

Although the metabolic differences identified in this study may solely be due to the disease process or reflect differences in normal cartilage and SF biology, it is more likely to be represented by a complex interplay of all these factors.

#### Potential of NMR and MS in further analysis of SF in health and disease

There are a few spectroscopic methods available to analyse metabolites and generate metabolic datasets for complex biological samples. <sup>1</sup>H-NMR spectroscopy produces a comprehensive profile of metabolic signals without derivatization, separation and pre-selected measurement parameters<sup>45</sup>.

In the past decade, <sup>1</sup>H-NMR-based metabolic profiling has developed into a powerful tool for the identification of metabolites and biochemical markers for a variety of human disorders<sup>46</sup>. Metabolic profiling of SF provides a direct representation of what is taking place in the joint and yields the most accurate and joint specific metabolic profile that is relevant to OA<sup>47</sup>.

There is some evidence in the literature that biomarkers exist in SF for numerous conditions including OA degradation products<sup>12,14,17–19,21,22</sup>, prosthetic joint infection<sup>48,49</sup>, and bacterial infection in native joints<sup>50</sup>. The techniques utilised in this study could be used in larger groups to further analyse the relevance of previously found biomarkers in joint disease and to identify new metabolic patterns of diseases such as OA and inflammatory arthritis.

Our study demonstrates the potential of metabolic profiling of joint fluid using NMR spectroscopy to identify important metabolites in these conditions.

At present the above speculations remain little more than hypotheses with a modicum of evidence already in the literature. Further studies should utilise a larger group of fluid samples with a more targeted analysis of individual metabolites for a specific patient group or disease category.

#### Limitations

Despite the samples in both groups being matched for age, gender, BMI, with similar medical comorbidities and ethnicity, the overall numbers were small (12 in each group). However, the validated O-PLS-DA model demonstrated 14 metabolites that were significantly different between the hip and knee groups, four of which remained significant following univariate testing and FDR adjustment. Secondly, there was no age/gender-matched non-arthritis control groups, although such samples would be difficult to acquire because of ethical constraints. Furthermore, this study did not take into account the number of compartments in the knee affected with OA. However, our unpublished analysis has not

demonstrated any metabolic differences between OA affecting one or more compartments.

#### Conclusion

To our knowledge, this is the first study to indicate differences in the metabolic profile of HSF between the hip and knee joints in patients with end-stage OA. There were four metabolites found in significantly greater proportions in the knee group (N-acetylated molecules, GAGs, citrate and glutamine). These metabolites have a role in collagen degradation, the TCA cycle and oxidative metabolism in diseased joints.

Further research is required with a larger group of patients and a control group to see if these metabolites may serve as putative biomarkers for the diagnosis of knee OA, monitoring of disease progression and/or future treatment strategies.

#### Author contributions

All authors made substantial contributions to the conception and design of the study, data acquisition and analysis, drafting/revision and final approval of the manuscript.

#### Competing interests

Professor John Lindon declares a shareholding in the company "Metabometrix Ltd" which is contracted to perform small molecule studies. Dr Claire Boulangé has received funding from "Metabometrix Ltd". No other authors disclose any competing interests.

#### Source of funding

No external funding was received for this study.

#### Acknowledgements

This article is independent research funded by the National Institute for Health Research (NIHR) and Imperial Biomedical Research Centre (BRC). The views expressed in this publication are those of the authors and not necessarily those of the National Health Service (NHS), the NIHR or the Department of Health.

#### Supplementary data

Supplementary data to this article can be found online at <https://doi.org/10.1016/j.joca.2019.07.017>.

#### References

1. Chen A, Gupte C, Akhtar K, Smith P, Cobb J. The global economic cost of osteoarthritis: how the UK compares. *Arthritis* 2012;2012:698709.
2. Krasnokutsky S, Attur M, Palmer G, Samuels J, Abramson SB. Current concepts in the pathogenesis of osteoarthritis. *Osteoarthr Cartil* 2008;16(Suppl 3):S1–3.

3. Yoshida H, Faust A, Wilckens J, Kitagawa M, Fetto J, Chao EY. Three-dimensional dynamic hip contact area and pressure distribution during activities of daily living. *J Biomech* 2006;39:1996–2004.
4. Andriacchi TP, Koo S, Scanlan SF. Gait mechanics influence healthy cartilage morphology and osteoarthritis of the knee. *J Bone Joint Surg Am* 2009;91(Suppl 1):95–101.
5. Galandakova A, Ulrichova J, Langova K, Hanakova A, Vrbka M, Hartl M, et al. Characteristics of synovial fluid required for optimization of lubrication fluid for biotribological experiments. *J Biomed Mater Res B Appl Biomater* 2017;105:1422–31.
6. Olszewska-Slonina D, Jung S, Matewski D, Olszewski KJ, Krzyzynska-Malinowska E, Braszkiewicz A, et al. Lysosomal enzymes in serum and synovial fluid in patients with osteoarthritis. *Scand J Clin Lab Investig* 2015;75:145–51.
7. Snelling SJ, Bas S, Puskas GJ, Dakin SG, Suva D, Finckh A, et al. Presence of IL-17 in synovial fluid identifies a potential inflammatory osteoarthritic phenotype. *PLoS One* 2017;12, e0175109.
8. Fischer K, Kettunen J, Wurtz P, Haller T, Havulinna AS, Kangas AJ, et al. Biomarker profiling by nuclear magnetic resonance spectroscopy for the prediction of all-cause mortality: an observational study of 17,345 persons. *PLoS Med* 2014;11, e1001606.
9. Holmes E, Loo RL, Stamler J, Bictash M, Yap J, Chan Q, et al. Human metabolic phenotype diversity and its association with diet and blood pressure. *Nature* 2008;453:396–400.
10. Yu B, Zheng Y, Nettleton JA, Alexander D, Coresh J, Boerwinkle E. Serum metabolomic profiling and incident CKD among African Americans. *Clin J Am Soc Nephrol* 2014;9:1410–7.
11. Lamers R-JAN, van Nesselrooij JHJ, Kraus VB, Jordan JM, Renner JB, Dragomir AD, et al. Identification of an urinary metabolite profile associated with osteoarthritis. *Osteoarthritis Cartilage* 2005;13:762–8.
12. Zhai G, Wang-Sattler R, Hart DJ, Arden NK, Hakim AJ, Illig T, et al. Serum branched-chain amino acid to histidine ratio: a novel metabolomic biomarker of knee osteoarthritis. *Ann Rheum Dis* 2010;69:1227–31.
13. Qiu Y, Cai G, Zhou B, Li D, Zhao A, Xie G, et al. A Distinct Metabolic Signature of Human Colorectal Cancer with Prognostic Potential. *Clinical Cancer Research*; 2014.
14. Zhang WD, Sun G, Likhodii S, Aref-Eshghi E, Harper PE, Randell E, et al. Metabolomic analysis of human synovial fluid and plasma reveals that phosphatidylcholine metabolism is associated with both osteoarthritis and diabetes mellitus. *Metabolomics* 2016;12:24.
15. Kim S, Hwang J, Kim J, Ahn JK, Cha HS, Kim KH. Metabolite profiles of synovial fluid change with the radiographic severity of knee osteoarthritis. *Jt Bone Spine* 2017 October;84:605–10.
16. Xu Z, Chen T, Luo J, Ding S, Gao S, Zhang J. Cartilaginous metabolomic study reveals potential mechanisms of osteophyte formation in osteoarthritis. *J Proteome Res* 2017;16:1425–35.
17. Zhang Q, Li H, Zhang Z, Yang F, Chen J. Serum metabolites as potential biomarkers for diagnosis of knee osteoarthritis. *Dis Markers* 2015;2015:684794.
18. Zhang W, Likhodii S, Zhang Y, Aref-Eshghi E, Harper PE, Randell E, et al. Classification of osteoarthritis phenotypes by metabolomics analysis. *BMJ Open* 2014;4, e006286.
19. Zhang W, Sun G, Likhodii S, Liu M, Aref-Eshghi E, Harper PE, et al. Metabolomic analysis of human plasma reveals that arginine is depleted in knee osteoarthritis patients. *Osteoarthritis Cartil* 2016;24:827–34.
20. Lindon JC, Nicholson JK. Spectroscopic and Statistical Techniques for Information Recovery in Metabonomics and Metabolomics, doi:10.1146/annurev.anchem.1.031207.113026. *Annual Review of Analytical Chemistry* 2008; 1: 45–69.
21. Damyanovich AZ, Staples JR, Chan ADM, Marshall KW. Comparative study of normal and osteoarthritic canine synovial fluid using 500 MHz <sup>1</sup>H magnetic resonance spectroscopy. *J Orthopaedic Res* 1999;17:223–31.
22. Lacitignola L, Fanizzi FP, Franciosi E. <sup>1</sup>H NMR investigation of normal and osteoarthritic synovial fluid in the horse. *Vet Comp Orthop Traumatol* 2008;21:85–8.
23. Hoppenfeld S, De Boer PG, Buckley R. *Surgical Exposures in Orthopaedics : The Anatomic Approach* 2009.
24. Dona AC, Jiménez B, Schäfer H, Humpfer E, Spraul M, Lewis MR, et al. Precision high-throughput proton NMR spectroscopy of human urine, serum, and plasma for large-scale metabolic phenotyping. *Anal Chem* 2014;86:9887–94.
25. Veselkov KA, Lindon JC, Ebbels TM, Crockford D, Volynkin VV, Holmes E, et al. Recursive segment-wise peak alignment of biological (1)H NMR spectra for improved metabolic biomarker recovery. *Anal Chem* 2009;81:56–66.
26. Dieterle F, Ross A, Schlotterbeck G, Senn H. Probabilistic quotient normalization as robust method to account for dilution of complex biological mixtures. Application in <sup>1</sup>H NMR metabonomics. *Anal Chem* 2006;78:4281–90.
27. van den Berg RA, Hoefsloot HC, Westerhuis JA, Smilde AK, van der Werf MJ. Centering, scaling, and transformations: improving the biological information content of metabolomics data. *BMC Genomics* 2006;7:142.
28. Wishart DS, Jewison T, Guo AC, Wilson M, Knox C, Liu Y, et al. HMDB 3.0—the human Metabolome database in 2013. *Nucleic Acids Res* 2013;41:D801–7.
29. Ulrich EL, Akutsu H, Doreleijers JF, Harano Y, Ioannidis YE, Lin J, et al. BioMagResBank. *Nucleic Acids Res* 2008;36:D402–8.
30. Cloarec O, Dumas ME, Craig A, Barton RH, Trygg J, Hudson J, et al. Statistical total correlation spectroscopy: an exploratory approach for latent biomarker identification from metabolic <sup>1</sup>H NMR data sets. *Anal Chem* 2005;77:1282–9.
31. Bartel J, Krumsiek J, Theis FJ. Statistical methods for the analysis of high-throughput metabolomics data. *Comput Struct Biotechnol J* 2013;4, e201301009.
32. Benjamini Y, Hochberg Y. Controlling the false discovery rate: a practical and powerful approach to multiple testing. *J R Stat Soc Ser B* 1995;57:289–300.
33. Posma JM, Robinette SL, Holmes E, Nicholson JK. MetaboNetworks, an interactive Matlab-based toolbox for creating, customizing and exploring sub-networks from KEGG. *Bioinformatics* 2014;30:893–5.
34. Kresse H, Schonherr E. Proteoglycans of the extracellular matrix and growth control. *J Cell Physiol* 2001;189:266–74.
35. Hardingham TE, Fosang AJ. Proteoglycans: many forms and many functions. *FASEB J* 1992;6:861–70.
36. Thompson Jr RC, Oegema Jr TR. Metabolic activity of articular cartilage in osteoarthritis. An in vitro study. *Journal of Bone and Joint Surgery - Series A* 1979;61:407–16.
37. Schiller J, Naji L, Huster D, Kaufmann J, Arnold K. <sup>1</sup>H and <sup>13</sup>C HR-MAS NMR investigations on native and enzymatically digested bovine nasal cartilage. *Magma* 2001;13:19–27.

38. Berg JMTJ, Stryer L. Amino acids are made from intermediates of the citric acid cycle and other major pathways. In: *Biochemistry*. New York: W H Freeman; 2002.
39. Handley CJ, Speight G, Leyden KM, Lowther DA. Extracellular matrix metabolism by chondrocytes 7. Evidence that L-glutamine is an essential amino acid for chondrocytes and other connective tissue cells. *Biochim Biophys Acta Gen Subj* 1980;627:324–31.
40. Blanco FJ, Lopez-Armada MJ, Maneiro E. Mitochondrial dysfunction in osteoarthritis. *Mitochondrion* 2004;4:715–28.
41. de Sousa EB, Dos Santos Junior GC, Aguiar RP, da Costa Sartore R, de Oliveira ACL, Almeida FCL, et al. Osteoarthritic synovial fluid modulates cell phenotype and metabolic behavior in vitro. *Stem Cell Int* 2019;2019:8169172.
42. Liu Y, Hou R, Yin R, Yin W. Correlation of bone morphogenetic protein-2 levels in serum and synovial fluid with disease severity of knee osteoarthritis. *Med Sci Monit : international medical journal of experimental and clinical research* 2015;21:363–70.
43. Catterall JB, Zura RD, Bolognesi MP, Kraus VB. Aspartic acid racemization reveals a high turnover state in knee compared with hip osteoarthritic cartilage. *Osteoarthritis Cartil* 2016;24:374–81.
44. Reyes C, Leyland KM, Peat G, Cooper C, Arden NK, Prieto-Alhambra D. Association between overweight and obesity and risk of clinically diagnosed knee, hip, and hand osteoarthritis: a population-based cohort study. *Arthritis & rheumatology (Hoboken, N.J.)* 2016;68:1869–75.
45. Nicholson JK, Wilson ID. High resolution proton magnetic resonance spectroscopy of biological fluids. *Prog Nucl Magn Reson Spectrosc* 1989;21:449–501.
46. Nagana Gowda GA, Raftery D. Can NMR solve some significant challenges in metabolomics? *J Magn Reson* 2015;260:144–60.
47. Adams Jr SB, Setton LA, Nettles DL. The role of metabolomics in osteoarthritis research. *J Am Acad Orthop Surg* 2013;21:63–4.
48. Parvizi J, Jacovides C, Antoci V, Ghanem E. Diagnosis of periprosthetic joint infection: the utility of a simple yet unappreciated enzyme. *J Bone Jt. Surg* 2011;93:2242–8.
49. Di Cesare PE, Chang E, Preston CF, Liu CJ. Serum interleukin-6 as a marker of periprosthetic infection following total hip and knee arthroplasty. *J Bone Joint Surg Am* 2005;87:1921–7.
50. Lenski M, Scherer MA. Diagnostic potential of inflammatory markers in septic arthritis and periprosthetic joint infections: a clinical study with 719 patients. *Infectious Diseases* 2015;47:399–409.